

THE PENNSYLVANIA STATE UNIVERSITY
MILLENNIUM SCHOLARS PROGRAM

DEPARTMENT OF BIOMEDICAL ENGINEERING

VISUALIZING MECHANOSENSORY CHANNELS FOR VASCULAR TRANSPORT IN
THE DURA

AMANDA M. CRAINE
SPRING 2019

A thesis
submitted in partial fulfillment
of the requirements
for a baccalaureate degree
in Biomedical Engineering

ABSTRACT

Migraines are one of the most common types of chronic pain humans endure, chronically impacting 10% of the global population¹. However, the mechanics of migraine formation are relatively unknown. Recent studies suggest that the dura mater may be related to migraine progression, location, and intensity². Additionally, studies suggest that mechanosensitive channels PIEZO1/2 along neurons in the brain also play a role in the migraine cascade³. PIEZO channels have been shown to utilize inflammatory responses, hemodynamic forces, and chemical changes to influence pain localization and duration^{3,4}. Therefore, we seek to visualize PIEZO channels in the dura of mice to understand the relation between changes in blood flow and neural stimulation that cause migraine pain.

First, a new dural dissection technique was developed to allow for evaluation of the dura's neurovascular network. PIEZO channels were co-stained along with markers for blood vessels and neurons via immunofluorescence staining and confocal imaging. PIEZO2 channels were shown to line the blood vessels of the dura, suggesting that PIEZO2 channels are activated by hemodynamic forces. Co-staining of PIEZO2 with neural markers β 3-tubulin and Neurofilament (NF) suggests a relation with axons. Further studies will be conducted to understand how PIEZO channels interact with specific regions of neurons. Other cells in the dura were also found to express PIEZO2. These cells have not been identified, but we hypothesize that they are mast cells. Additional studies will be conducted to confirm the cell origin.

Overall, this study allows us to define mechanosensitive channels PIEZO1/2 in the dura in addition to a novel approach to dural dissection. By establishing the presence of PIEZO

channels, in vivo studies can be conducted to understand how the channels interact with adjacent vessels and neurons to facilitate neurovascular coupling.

TABLE OF CONTENTS

LIST OF FIGURES	5
ACKNOWLEDGEMENTS	6
Chapter 1: Introduction	7
Section 1.1: Neurovascular Coupling	7
Section 1.2: Anatomy of the Dura	8
Section 1.3: Mechanosensory Channels	11
Section 1.4: Physiological Significance of Mechanosensory Channels	12
Chapter 2: Methods	14
Section 2.1: Perfusion	14
Section 2.2: Tissue Sectioning	14
Section 2.3: Dural Dissection	14
Section 2.4: Immunohistochemical Staining	15
Section 2.4.1: PIEZO1 Study	15
Section 2.4.2: PIEZO2 Study	16
Section 2.5: Imaging	18
Chapter 3: Results	19
Section 3.1: PIEZO1 Results	29
Section 3.2: PIEZO2 Results	20
Chapter 4: Discussion	24
Section 4.1: PIEZO1 Discussion	24
Section 4.2: PIEZO2 Discussion	24
Section 4.3: Future Work	26
SUPPLEMENTARY MATERIAL	28
BIBLIOGRAPHY	29

LIST OF FIGURES

Figure 1: Arterial Dilation Increases Blood Volume, Flow, and Oxygenation.	7
Figure 2: Anatomy of the Cranial Meninges.	8
Figure 3: Venous and Arteriolar Vascularization in the Whole Mouse Dura.	9
Figure 4: Ascending Neuronal Pathways of the Trigeminovascular System.	10
Figure 5: PIEZO-Dependent Mechanotransduction.	11
Figure 6: Immunofluorescent Staining of PIEZO1 and AQP4 in the Brain.....	19
Figure 7: Immunofluorescent Staining of PIEZO2 and Aquaporin-1 (AQP1) in the Liver	19
Figure 8: Immunofluorescent Staining of PIEZO2 and Aquaporin-1 (AQP1) in the Lung	20
Figure 9: Immunofluorescent Staining of PIEZO2 and Phalloidin in the Dura.	21
Figure 10: Immunofluorescent Staining of PIEZO2 and β 3-Tubulin in the Dura.....	21
Figure 11: Immunofluorescent Staining of PIEZO2 and NF in the Dura.....	22
Figure 12: Immunofluorescent Staining of PIEZO2 and CD117 in the Dura.	22
Figure 13: DAB and Toluidine Blue Staining of PIEZO2 and Mast Cells in the Dura.....	23
Figure 14: Cell Shape Comparison Between Observed Cells and Mast Cells.	25
Supp. Figure 1: Immunofluorescent Staining of MAP2 and Neurofilament (NF) in the Dura ...	28

ACKNOWLEDGEMENTS

I would like to thank Dr. Drew for the opportunity to work in his laboratory over the past four years. I am extremely grateful for the support that helped me grow from a novice to a more independent researcher, which helped me gain the confidence that I could pursue this novel project. I would also like to thank Jordan Norwood for training me in lab techniques, for being a great graduate student mentor. Finally, I'd like to thank the rest of the Drew Lab for being a welcoming environment for an undergraduate researcher to openly share thoughts and ask questions.

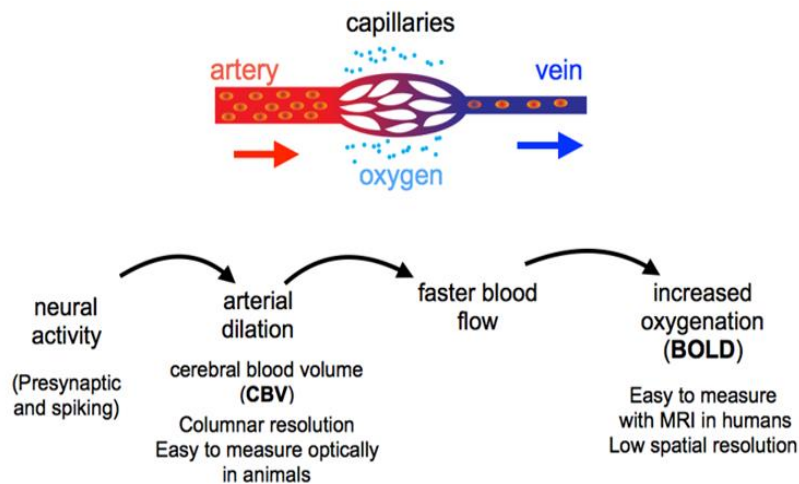
I would also like to thank Penn State's Millennium Scholars Program for providing me the tools and skills necessary for me to pursue my professional goals. Through the program's support and resources, I have been able to excel as an undergraduate student and peer mentor, while preparing for the next stage of my education and career.

Chapter 1

Introduction

Section 1.1: Neurovascular Coupling

The relationship between local neural activity and blood volume, neurovascular coupling (NVC), is used to non-invasively infer neural circuit dynamics in humans and model organisms. Figure 1 describes this relationship: as synapses activate and the electrical cascade travels down neurons, local arteries dilate, which increases cerebral blood volume (CBV)⁵. As CBV increases, there are more red blood cells present and oxygen uptake in the blood increases as a result. Imaging modalities that rely on oxygen concentration, such as functional magnetic resonance (fMR) imaging, utilize NVC to generate clear images of blood flow through the brain to help diagnose neurological abnormalities.



Adapted from Drew Lab.

Figure 1: Arterial dilation increases blood volume, flow, and oxygenation.

While NVC plays an essential role in studying neural activity in the brain, it is unclear if a similar network is present in the dura. In this study, we seek to define, visualize, and understand the mechanosensory channels related to the vascular network of the dura.

Section 1.2: Anatomy of the Dura

As a protective layer, the brain and spinal cord are enveloped by three membranes referred to as the meninges to isolate and stabilize the central nervous system^{6,7}. The dura mater (commonly called the dura) is the outermost layer on the meninges, sitting between the skull and the arachnoid mater, as seen in Figure 2⁷. The dura consists of two layers; the periosteal layer is the outer layer that is firmly attached to the skull, and the meningeal layer in the inner layer that touches the arachnoid mater and is continuous with the spinal dura⁷. This region contains the meningeal arteries that branch from the carotid artery and feed blood to the dura⁷. The inner, meningeal layer lays along the arachnoid layer and is continuous with the spinal dura⁷. The dura

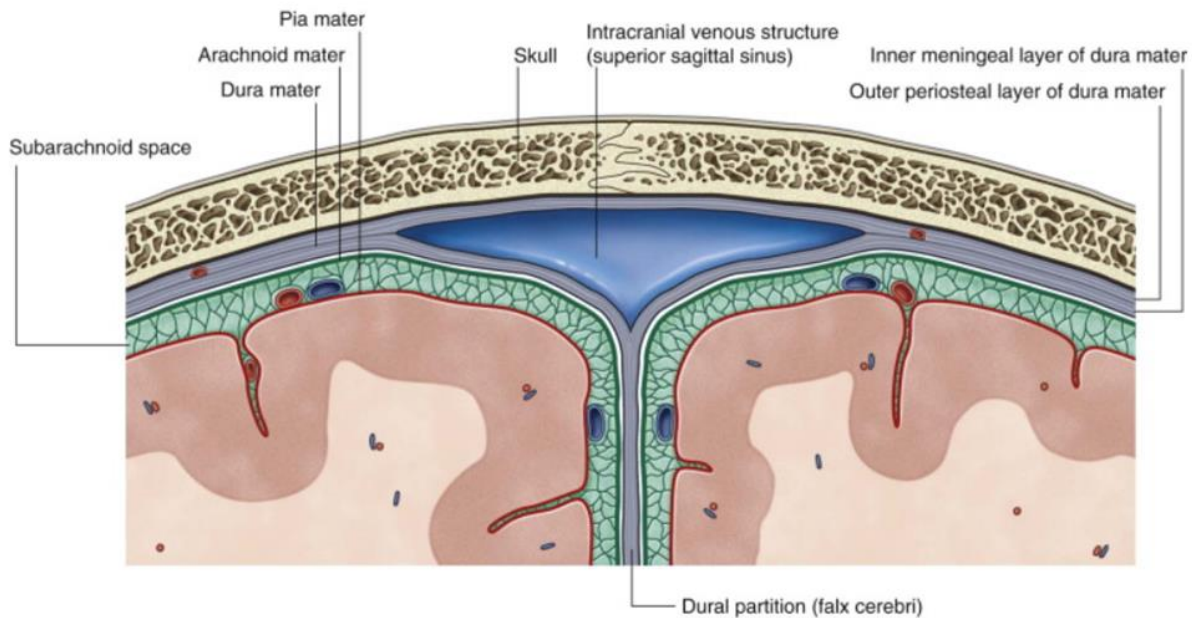


Figure 2: Anatomy of the Cranial Meninges.

Adapted from Drake et. al. 2015.

is well-innervated, with connections to both lymphatic and vascular systems^{6,7}. While the vasculature of human dura is well described, understanding vascularization in a mouse model is still vague.

In Figure 3, Mecheri et. al. presented the cartography of the main venous and arteriolar vessels in the whole mouse dura. The group found that occipital region is generally accompanied by venules (1) that run either closely to an arterial vessel (2) or a distance parallel to it (3).

However, some venules are not closely related to an arterial vessel (4). Most venous blood flows through the superior sagittal sinus (SSS) (5) or the transverse sinus (TS) (6), yet some follow to

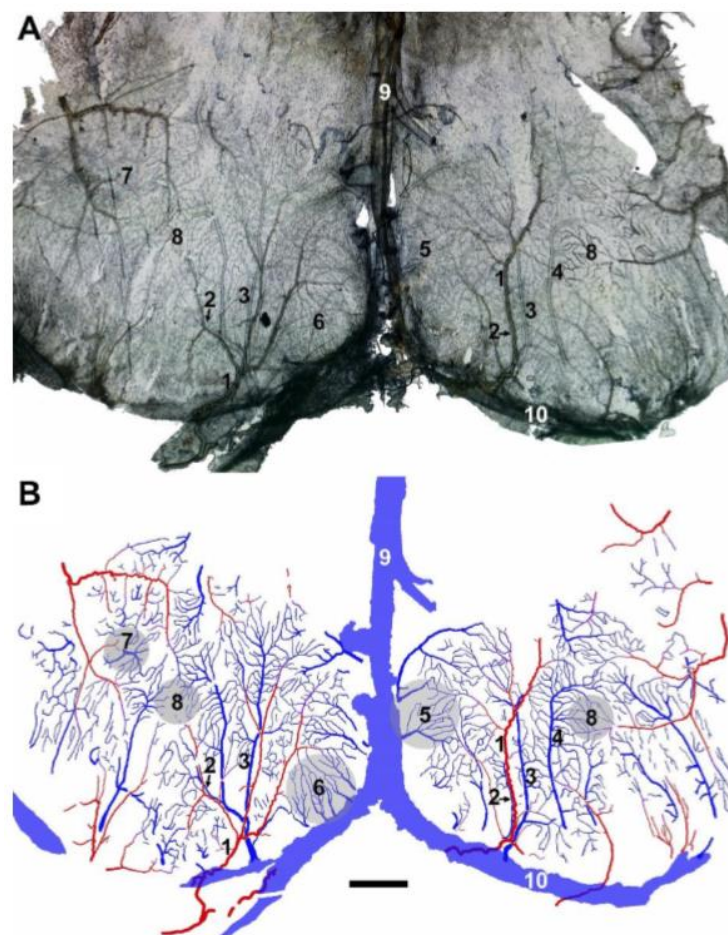


Figure 3: Venous and Arteriolar vascularization in the whole mouse dura.

Arterioles are shown in red and veins shown in blue. Capillaries are partially drawn. **A)** Original dural preparation. **B)** Drawing of the main vascular system.

the frontolateral region of the dura (7). Capillary beds are represented by (8). The SSS is represented by (9), and the TS is represented by (10)⁶.

Dural function may play a significant role in migraine and pain development

Migraine physiology is complex and understudied; it is known that migraine development involves brain excitability, intracranial arterial dilation, recurrent activation, and sensitization of the trigeminovascular pathway². In the trigeminovascular system, neurons in the trigeminal nerve innervate cerebral blood vessels. Figure 4 shows the ascending neuronal pathway of the trigeminovascular system involved in migraine development. Dura-sensitive neurons that project

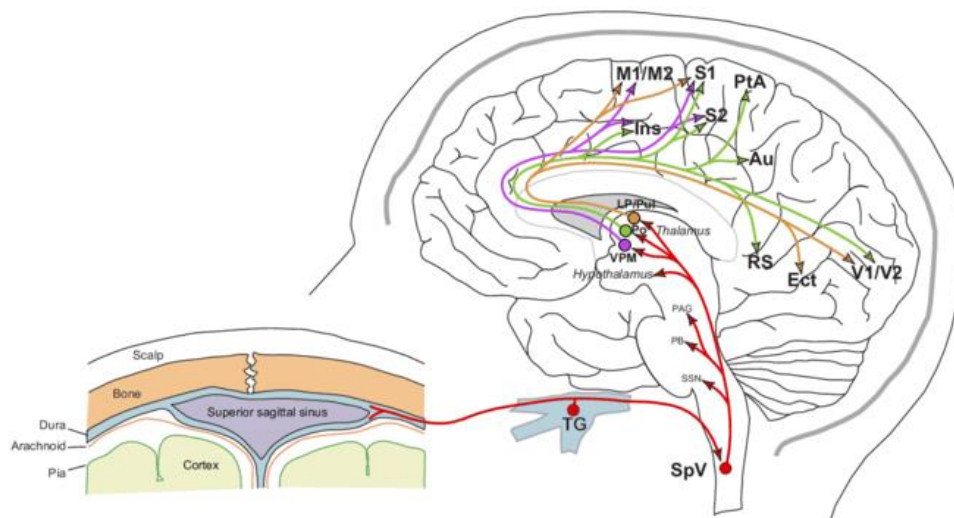


Figure 4: Ascending neuronal pathways of the trigeminovascular system.
Trigeminal neurons related to migraine and their respective paths through the brain.

to the trigeminal area of the somatosensory cortex (seen in red) suggest that the dura is important in defining migraine location, intensity, and quality of pain². Additionally, dura-sensitive neurons that project to other areas of the brain suggest the dura is also involved in non-pain related migraine symptoms like motor clumsiness, difficulty focusing, transient amnesia, and photophobia².

On the vascular side, the headache associated with a migraine attack is thought to be activated partially by dural vessels via mechanical, electrical, or chemical stimulation². However, there has been debate over whether vascular changes have a primary role in migraine development. We seek to understand how the dura behaves to mechanical stimulation and its relation to the neurovascular pathway. Therefore, we can build a framework for characteristics of the dura that provide important roles in pain and migraines.

Section 1.3: Mechanosensory Channels

Ion channels with mechanosensory properties are present in the lungs and gastrointestinal tract; they are known to assist with both respiration and intraluminal pressure changes that affect urine flow^{8,9}. Therefore we can infer that there are mechanosensory channels that relate neurovascular pressure changes to electrical impulses in the brain and the dura.

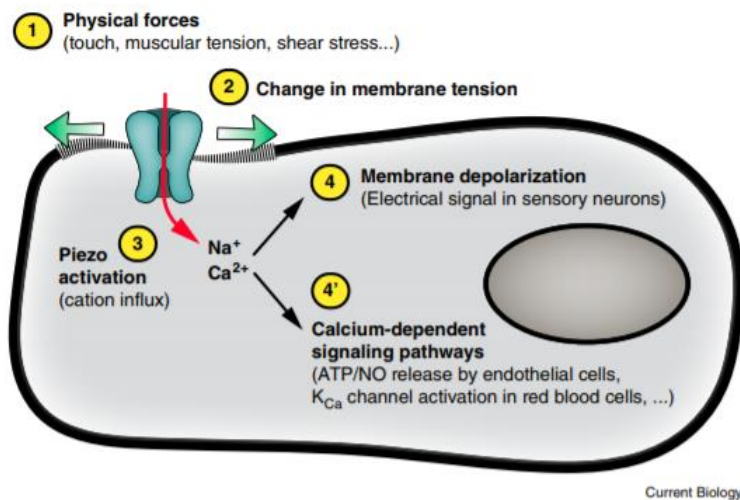


Figure 5: PIEZO-dependent mechanotransduction.

The process in which PIEZO channels uptake mechanical forces to produce electrical outputs.

PIEZO1 and PIEZO2 are mechanically-activated ion channels that mediate touch, proprioception, and vascular development¹⁰. Figure 5 provides visualization of how PIEZO

channels function¹¹. When exposed to a mechanical stimulus, the cell membrane experiences tensile changes that activate the PIEZO channel¹¹. The stimuli in vivo are usually shear stresses, yet the amount of force required to gate the channels is unknown¹¹. When PIEZO channels are activated, cations like Na⁺, K⁺, Mg²⁺, and Ca²⁺ can permeate into the cell, therefore inducing membrane depolarization¹¹. Figure 5 specifically shows the potential for PIEZO channels to activate Ca²⁺ signaling pathways.

Recent studies have shown that PIEZO1 is a shear stress sensor necessary for proper vascular endothelial development in mice^{12,13}. Absence of PIEZO1 was found to be particularly detrimental to vascular stability, which ultimately affects the path of blood through the body¹². PIEZO2, another mechanosensory protein derived from the same gene as PIEZO1, is mainly expressed in somatosensory neurons. Therefore, the main physiological role of PIEZO2 is to maintain detection of pain, touch, and proprioception (awareness of position or movement of the body)^{10,11}. Additionally, PIEZO2 is essential in sending mechanical signals from lung inflation to the sensory neurons that control respiration⁹.

In this study, the goal is to visualize the presence of PIEZO1 and PIEZO2 in the dura of mice to relate the mechanical stresses associated with fluid flow through the brain to the electrical impulses that allow the brain to control our nervous system.

Section 1.4: Physiological Significance of Mechanosensory Channels

Prior to the discovery of PIEZO channels, some studies found that the presence of mechanosensitive receptors in meningeal nociception, detection of painful stimuli, could be related to pulsating pain and mechanical allodynia³. Pulsating pain is a common symptom of

migraine, occurring in 70% of cases; mechanical allodynia is pain induced by a light stimulus and occurs in 90% of migraine cases³. Since the discovery of PIEZO channels, there have been multiple studies that suggest that PIEZO channels are essential in migraine pain development.

PIEZO1/2 channels have been discovered in the trigeminal ganglia of both the rat and mouse³. Activation of these channels along individual neurons can trigger pain generation in the meninges³. Further, PIEZO1 receptors can generate nociceptive spiking activity via temporal summation of pain signals on neurons to the brainstem, which shows that PIEZO channels may aid in migraine pain localization as well as pain intensity³. Elevated currents related to PIEZO2 channels were shown to induce an inflammatory response involved in mechanical allodynia and hyperalgesia, an increased sensitivity to pain⁴. Since hyperalgesia is related to vasoactive immune response endothelium-1, it is probable that PIEZO2 is the main mechanotransducer in endothelial cells that utilize physical changes by the vasoactivity to facilitate hyperalgesia⁴.

While it has been suggested that both the neurovascular components of the dura and mechanosensitive channels are associated with pain development, these channels have not been extensively studied in the dura. Therefore, we seek to visualize the PIEZO1/2 expression in the dura to eventually understand if these components of the migraine cascade work together in developing pain.

Chapter 2

Methods

Section 2.1: Perfusion

Intracardial perfusions were performed on Swiss Webster mice. Mice were first anesthetized with isoflurane with continuous exposure throughout the perfusion. Using scissors, an incision was made starting from the central abdomen to the diaphragm. The thoracic cavity was opened by creating lateral incisions through the ribs, to expose the heart. The pericardium was removed, a 21-gage needle attached to an infusion pump was injected into the left ventricle. The mice were perfused with a heparinized saline, then 4% paraformaldehyde (PFA). The dura, liver, lungs, and brain were saved. Dural tissue was immediately placed into PBS. Liver, brain, and lung tissue was placed into 4% PFA for one day, then 30% sucrose for two days.

Section 2.2: Tissue Sectioning

The liver, brain, and lung tissues were removed from the 30% sucrose. Tissue was sectioned into 100 μm samples using the freezing microtome.

Section 2.3: Dural Dissection

After perfusion, the mouse was placed in the prone position and the head was severed using scissors. The skin was removed from the skull and the tip of the nose was removed to expose the nasal cavity. An axial cut was made through the nasal cavity, mandibular junction, and lateral regions of the skull. A coronal cut was made at the posterior end of the skull to expose the caudal side of the brain. Once the axial cuts were complete, the dorsal and ventral sides of the skull were separated and the ventral side was removed. The dura is located on the interior lining of the

skull. A blunt tool was used to remove the brain from the dorsal side to expose the dura. Dural dissection began by locating the web of transparent tissue towards the anterior region. Using tweezers, the tissue was gently peeled from the bone. Dura was added to PBS and immunofluorescence began 1-4 days after dissection.

Section 2.4: Immunofluorescence

Section 2.4.1: PIEZO1 Study

Finding PIEZO1 in the Dura

The optimal PIEZO1 concentration was identified using the hippocampal region of the brain as a positive control prior to dural staining⁹. Control samples were stained in 24 cell wells with one section per well. Tissue was washed in PBS for 5 minutes, then PBS was removed and the blocking solution (4% goat serum and PBS-T) was added for 1 hour. Once the blocking solution was removed, the samples were washed in PBS and placed in the primary antibody solution overnight at 4°C. PIEZO1 (Invitrogen - Rabbit) was studied at 1:20 and 1:50 dilutions along with 1:250 dilution of Aquaporin-4 (Santa Cruz - Mouse). Since our AQP4 antibody had already been validated and the expression of AQP4 in the brain is known, it was used as a positive staining control. Once the primary solution was removed, the samples had two PBS washes, then placed in the secondary antibody solution overnight in the 4° refrigerator at 1:500 dilution for each sample. Goat Anti-Rabbit (Alexa Fluor® 488) bound to PIEZO1 and Goat Anti-Mouse (Alexa Fluor® 647) bound to Aquaporin-4. The next day, the secondary solution was removed and the samples were washed in PBS three times. After the last wash, the samples were mounted onto glass slides relative to the PIEZO1 concentration and the slides were placed in the 37° incubator

overnight. Once the samples were dry, the slides were coverslipped using DAPI and placed back into the incubator overnight. The optimal PIEZO1 antibody dilution was determined to be 1:20.

To study PIEZO1 in relation to the vascular and neural networks in the dura, dura samples were first mounted on glass slides after dissection and placed in the 37° incubator to dry overnight. Fluorescence staining proceeded as explained above using blocking with 4% goat serum. The primary antibodies and their respective dilutions used were PIEZO1 (1:20) and Neurofilament (Santa Cruz, 1:250). Secondary antibodies used at 1:500 dilution were Goat Anti-Rabbit (Alexa Fluor® 488) and Goat Anti-Mouse (Alexa Fluor® 647). After staining, the samples were coverslipped using DAPI.

Section 2.4.2: PIEZO2 Study

Finding PIEZO2 in the Dura

The optimal PIEZO2 concentration was identified using a positive and negative control prior to dural staining. Lung tissue was used as the positive control while liver tissue was used as the negative control⁹. Control samples were stained with the same method as the PIEZO1 study. Three separate PIEZO2 (Invitrogen) primary dilutions were initially studied: 1:100, 1:250, and 1:500 along with 1:250 dilution of Aquaporin-1 (Santa Cruz). Our AQP1 antibody had already been validated and the expression of AQP1 in the liver and lung is known, therefore it was used as a positive staining control. Secondary antibodies Goat Anti-Rabbit (Alexa Fluor® 488) bound to PIEZO2 and Goat Anti-Mouse (Alexa Fluor® 647) bound to Aquaporin-1. The optimal PIEZO2 antibody dilution was determined to be 1:250.

To study PIEZO2 in dura, samples were first mounted on glass slides, then stained. Slide staining was more advantageous than cell well staining because we can avoid tissue perturbation during well staining. The dura in a mouse model is also thin enough (~20-40 μm) to allow staining directly on the slide. The primary antibodies and their respective dilutions used were PIEZO2 (1:250) and Neurofilament (Santa Cruz, 1:250). Secondary antibodies used at 1:500 dilution were Goat Anti-Rabbit (Alexa Fluor® 488) and Goat Anti-Mouse (Alexa Fluor® 647). After staining, the samples were coverslipped using DAPI.

Staining for Mast Cell Detection in the Dura

To determine the presence of mast cells in the dura, CD117 expression was first evaluated in the brain to determine the proper dilution. Fluorescence staining was completed in 24 cell wells. Samples were blocked with 4% goat serum, primary antibodies used were CD117 (Santa Cruz, 1:100, 1:250, 1:500), and Aquaporin-4 (1:250). Secondary antibodies at 1:500 dilution were Goat Anti-Rat (Alexa Fluor® 488) and Goat Anti-Mouse (Alexa Fluor® 647). Samples were mounted and coverslipped using DAPI.

Mast cells were studied using a 3,3'-diaminobenzene (DAB) staining technique with a Toluidine Blue dye (abcam). Dura samples were dissected and mounted onto glass slides as described above. The DAB staining for Mouse and Rabbit-Specific HRP/DAB Detection protocol was used. All solutions used came from the abcam DAB staining kit. Once mounted, dura was incubated for ten minutes in the Hydrogen Peroxide Block. After four washes in PBS, the Protein Block was added for five minutes. After another one wash in PBS, the primary antibody solution with PIEZO2 (1:250) was added and the samples were incubated overnight. The following day,

dura samples were washed in PBS four times. Samples were then incubated in the Anti-Mouse and Rabbit solution for ten minutes, followed by four PBS washes. Streptavidin Peroxidase was added for ten minutes followed by four rinses in PBS. Under a fume hood, the DAB solution (20 μ L DAB Chromagen and 1 mL DAB Substrate) was added to the samples and incubated for ten minutes. The samples were then rinsed in PBS four times.

Instead of following the standard DAB protocol for staining using Hematoxylin, toluidine blue was used to stain mast cells. The NovaUltra Special Stain Kit protocol was used for toluidine blue staining. Samples were stained in 200 μ L toluidine blue working solution (5 mL toluidine stock solution, 45 mL 1% NaCl, pH 2.3-2.5) for about three minutes, then washed in DI water three times. Then samples were dehydrated quickly in 95% ethanol and twice in 100% ethanol (ten dips for 95%, 20 dips for 100%). Samples were then cleared in xylene twice for three minutes. Samples were then coverslipped using Fluoromount.

Section 2.5: Imaging

Samples were investigated with a fluorescent microscope and imaged via confocal microscopy. Images were edited through ImageJ. Samples stained in DAB were imaged on QImaging Retiga 2000R CCD Camera.

Chapter 3

Results

Section 3.1: PIEZO1 Results

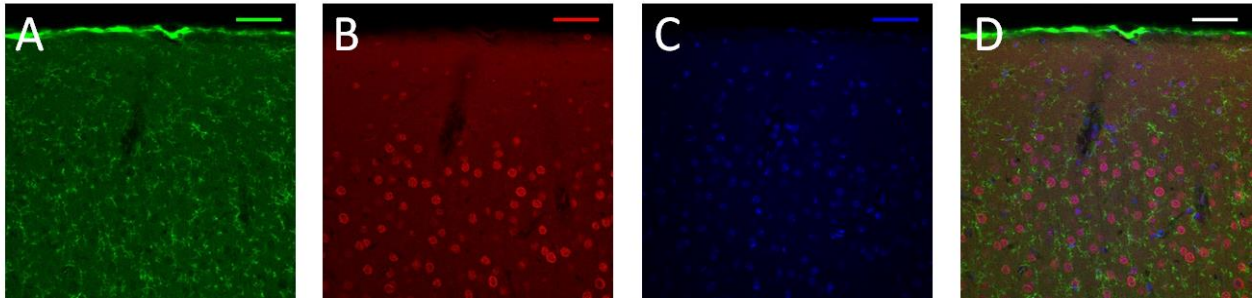


Figure 6: Immunofluorescent Staining of PIEZO1 and AQP4 in the Brain
PIEZO1 (green), AQP4 (red), DAPI (blue). Scale bars 50µm. A-D) 40x Magnification.

PIEZO1 expression was first validated in the murine brain as a positive control. Since there is heterogeneity between cell types stained by PIEZO1 and AQP4, PIEZO1 is present in the brain.

Section 3.2: PIEZO2 Results

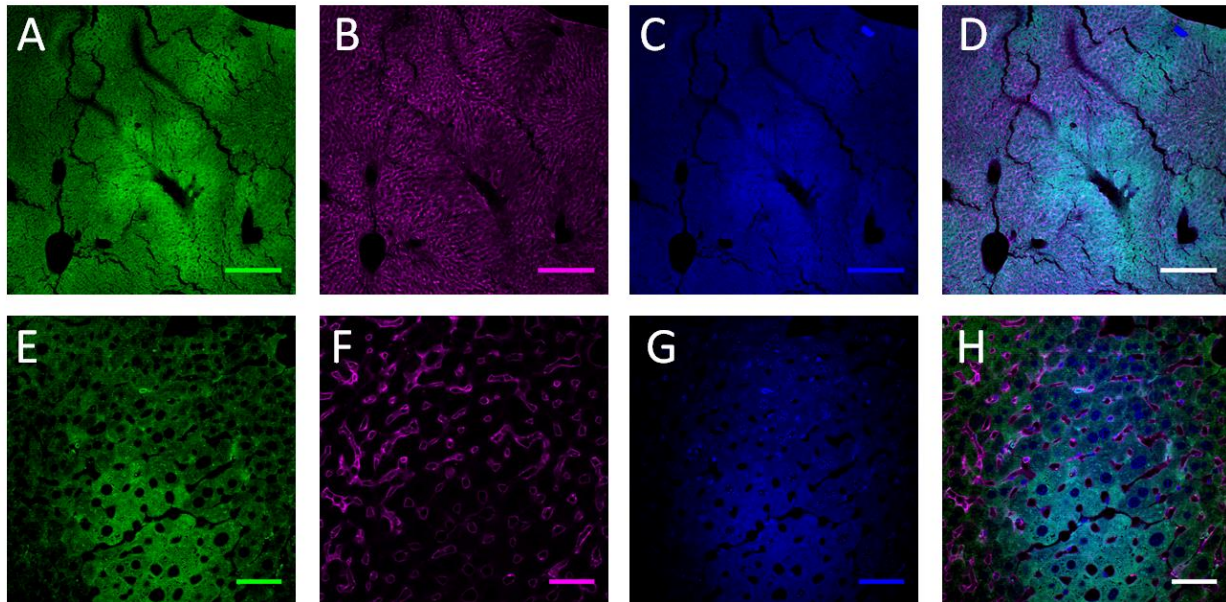


Figure 7: Immunofluorescent Staining of PIEZO2 and Aquaporin-1 (AQP1) in the Liver
PIEZO2 (green), AQP1 (pink), DAPI (blue). Scale bars 50µm. A-D) 10x Magnification. E-H) 40x Magnification.

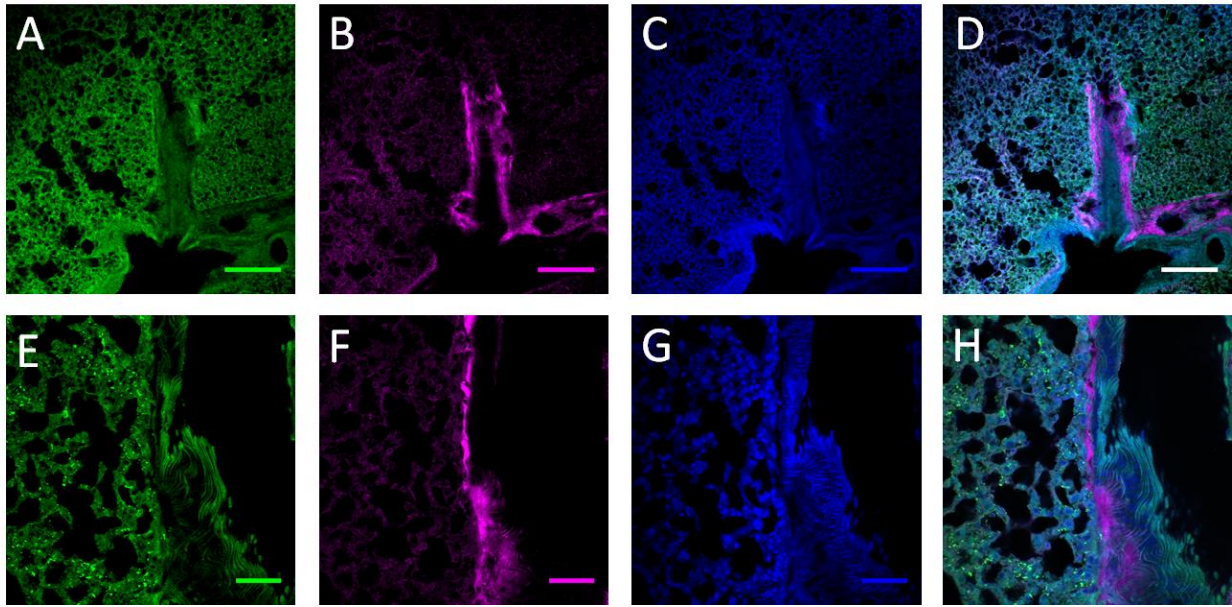


Figure 8: Immunofluorescent Staining of PIEZO2 and Aquaporin-1 (AQP1) in the Lung
 PIEZO2 (green), AQP1 (pink), DAPI (blue). Scale bars 50 μ m. **A-D)** 10x Magnification. **E-H)** 40x Magnification.

PIEZO2 expression was first evaluated in murine liver and lung (negative and positive control respectively) samples. Figure 7 shows a lack of PIEZO2 expression in the liver, while Figure 8 shows PIEZO2 expression in the lung. Figure 9 shows co-staining of PIEZO2 and Phalloidin, an actin filament (f-actin) marker, to visualize the relation between PIEZO2 channels and dural vasculature (specifically arteries). Co-staining is presented in yellow in D and H when the fluorescence of PIEZO2 and Phalloidin are merged together. To evaluate the connection between PIEZO2 channels and the neurons in the dura, PIEZO2 was co-stained with β 3-tubulin, an axon marker¹⁴, and Neurofilament (NF), a neural cytoplasm marker. Figures 10 and 11 show PIEZO2 staining along a dural vessel and neurons, especially the neurons in close proximity to the vessel. Co-staining of PIEZO2 and NF is clear in the cells lining the vessel presented in the 40x and 100x images, yet PIEZO2 is not expressed along the neurons where NF is expressed. Results from NF troubleshooting can be found in Supplemental Figure 1.

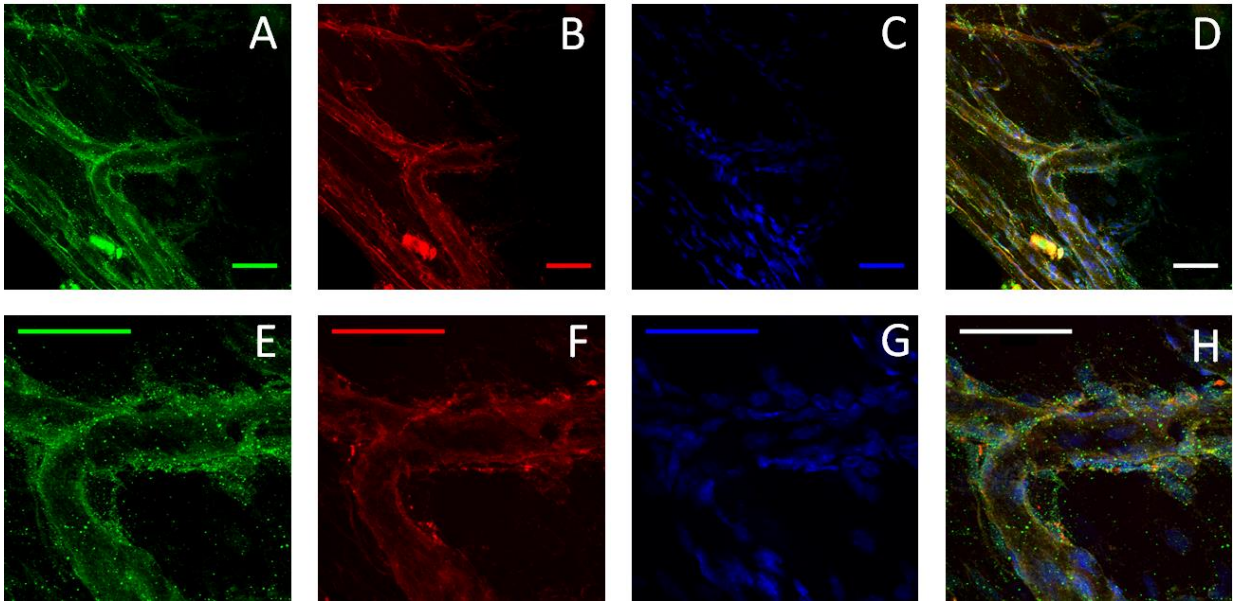


Figure 9: Immunofluorescent Staining of PIEZO2 and Phalloidin in the Dura.
 PIEZO2 (green), Phalloidin (red), DAPI (blue). Scale bars 50 μm . **A-D)** 40x Magnification. **E-H)** 100x Magnification

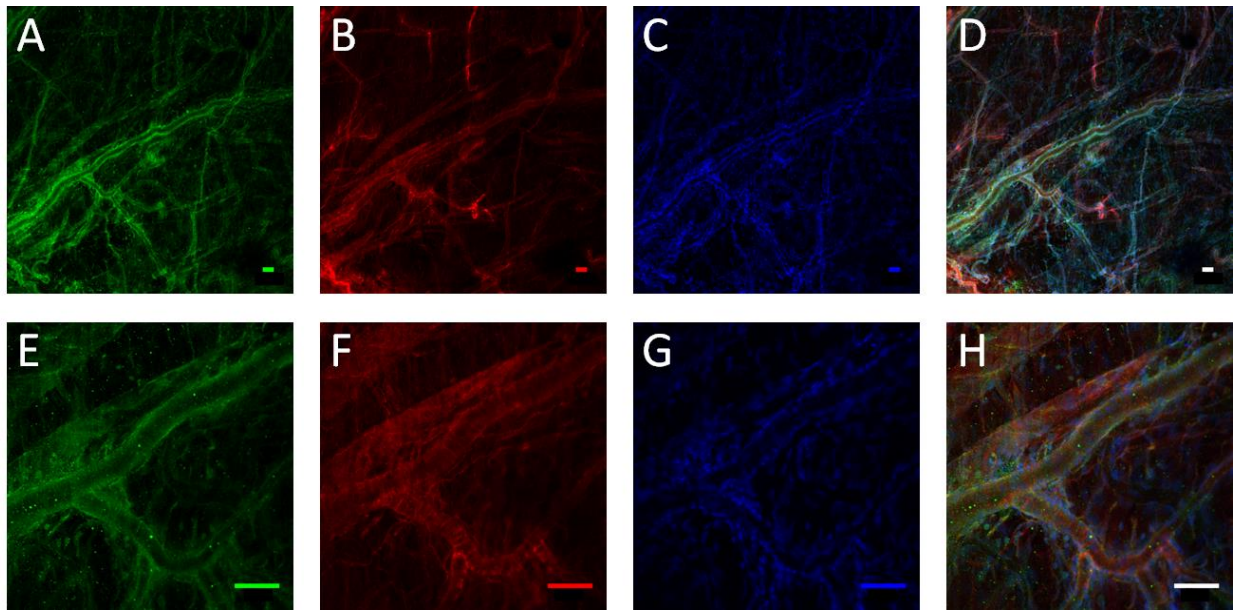


Figure 10: Immunofluorescent Staining of PIEZO2 and β 3-Tubulin in the Dura.
 PIEZO2 (green), β 3-tubulin (red), DAPI (blue). Scale bars 50 μm . **A-D)** 10x Magnification. **E-H)** 40x Magnification

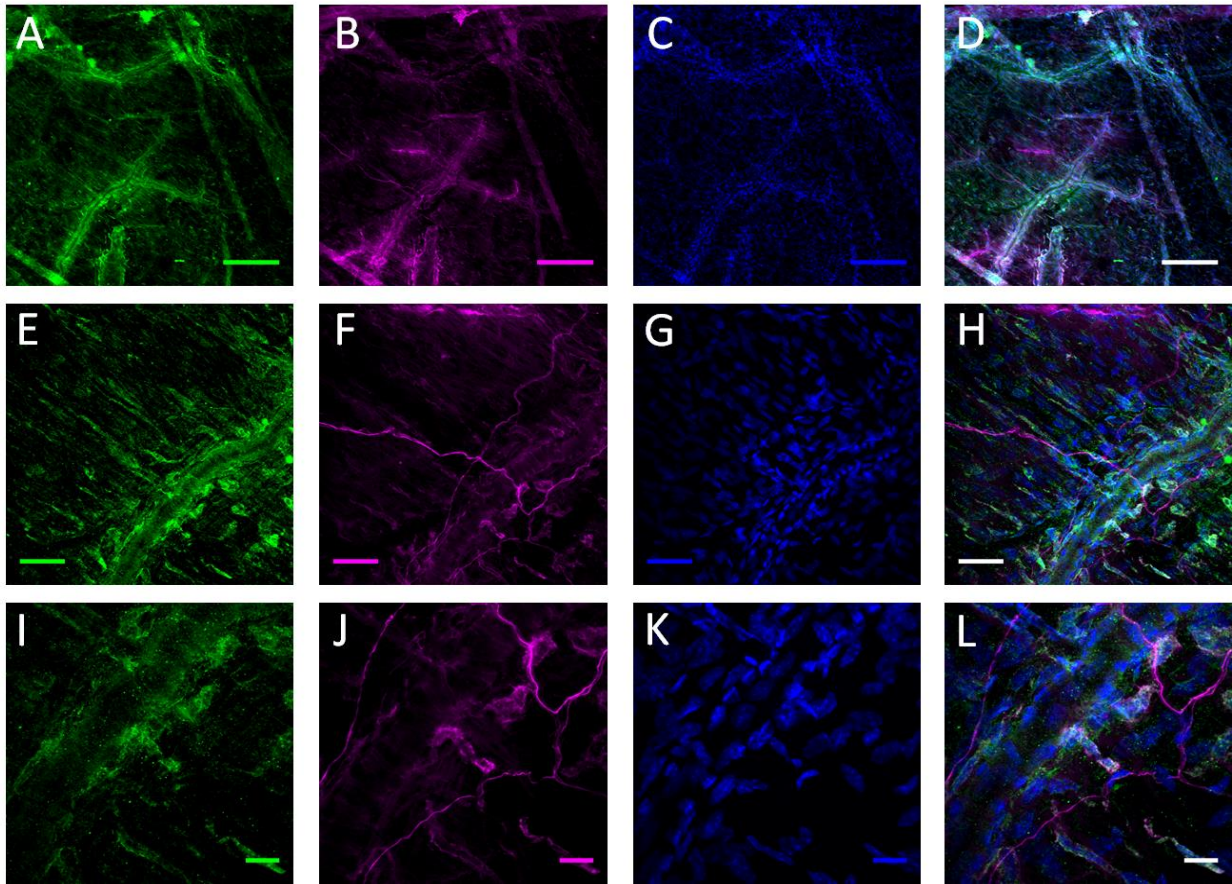


Figure 11: Immunofluorescent Staining of PIEZO2 and NF in the Dura.

PIEZO2 (green), NF (pink), DAPI (blue). **A-D**) 10x Magnification. Scale bar 50 μ m **E-H**) 40x Magnification. Scale bar 50 μ m. **I-L**) 100x Magnification. Scale bar 15 μ m

Co-staining of PIEZO2 and CD117, a mast cell marker, is present in Figure 12. However, co-staining is only present along the vessel; CD117 is not present in the cells and neurons that express PIEZO2. DAB staining with toluidine blue in Figure 13 does stain cells in the dura, but their origin is unknown. Potential mast cells are circled in red.

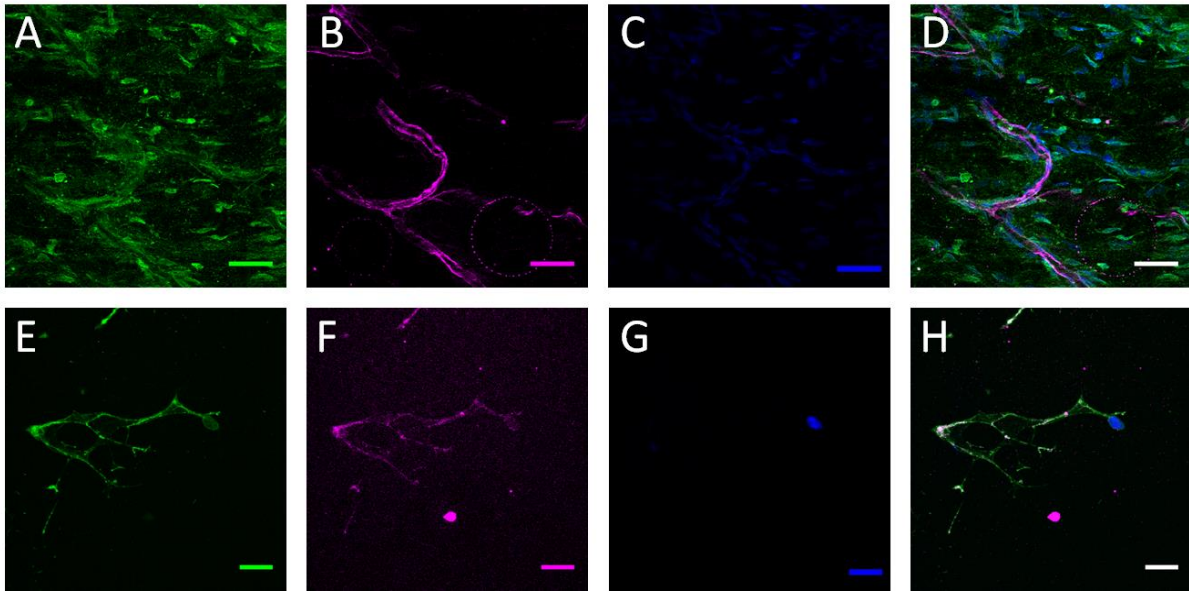


Figure 12: Immunofluorescent Staining of PIEZO2 and CD117 in the Dura.
 PIEZO2 (green), CD117 (pink), DAPI (blue). Scale bar 15 μ m. **A-D)** 40x Magnification. **E-H)** 100x Magnification. Scale bar 50 μ m.

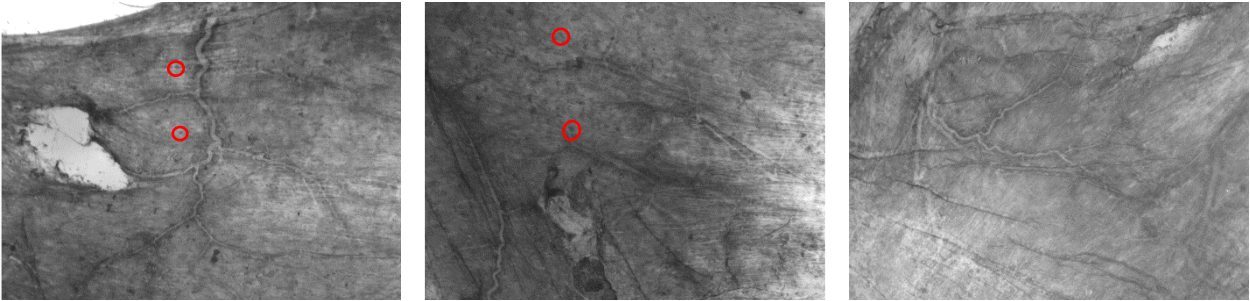


Figure 13: DAB and Toluidine Blue Staining of PIEZO2 and Mast Cells in the Dura.
 Three different dura samples presented; circled cells indicate potential mast cells. 8x magnification.

Chapter 4 Discussion

Section 4.1: PIEZO1 Studies

PIEZO1 control staining allowed us to validate the PIEZO1 antibody and define the proper dilution for immunohistochemical staining. It is clear that the morphology of the cells stained by PIEZO1 and AQP4 are different. In image A, PIEZO1 is likely expressed in neuropil, which is known to be high in PIEZO1¹¹. In image B, AQP4 is likely staining glial cells. While AQP4 is also known to stain neuropil as well, the cell shape seen in image B closely resonates with glial cells¹⁵. Since the cell types stained by PIEZO1 and AQP4 are different, we can define PIEZO1 expression in the brain.

While we have been able to define the dilution of PIEZO1 for tissue staining, attempts at dural studies have not yet been successful. The cause of the failed experiments is still unknown, and additional studies will be required to map PIEZO1 expression in the dura.

Section 4.2: PIEZO2 Studies

PIEZO2 control staining allowed us to validate the PIEZO2 antibody and define the proper dilution for immunohistochemical staining. Initially, Figure 5 seems to show positive PIEZO2 expression in the liver. However, there is little cellular heterogeneity across the antibody expression in the tissue. Therefore, we can infer that the PIEZO2 staining in the liver is only autonomous fluorescence and not actual PIEZO2 expression. In Figure 6, PIEZO2 expression is present in the lung which can be validated by literature stating the role of PIEZO2 in respiration. Expression is clear in image E, where there are small clusters of PIEZO2 expression in the lung

tissue adjacent to the endothelial cells lining the airway in the center of the figure (as seen in image F).

Co-staining of PIEZO2 and Phalloidin suggests that PIEZO2 channels line the blood vessels in the dura, particularly the arteries. This is especially seen in the arterial bifurcation focused in images E-F of Figure 7. Therefore, it is possible that PIEZO2 responds to the mechanical hemodynamic forces from blood vessels. Co-staining of PIEZO2 and β 3-tubulin is present along the neuron on the right side of images A-D in Figure 8. However, co-staining between PIEZO2 and NF is unclear. While co-staining with β 3-tubulin may suggest that PIEZO2 applies energy from hemodynamic forces to produce an electrical stimulus, more studies must be conducted to confirm this relation.

In images E and I of Figure 9, PEIZO2 also stains unknown cells in the dura. It is possible that they are mast cells, which would indicate that the dura plays a role in the inflammatory response and that mast cells may be important in migraine treatment. Figure 10 shows the similarities in cell shape between our PIEZO2 studies and previous mast cell anatomy studies¹⁶. Image A is the PIEZO2 cell staining data from the PIEZO2+CD117 study presented in Figure 9. Image B is the

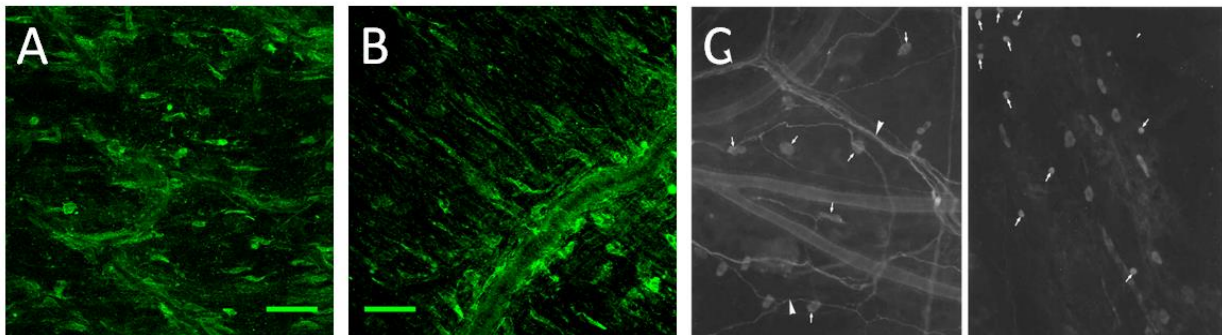


Figure 14: Cell shape comparison between observed cells and mast cells.

A) PIEZO2 stain from PIEZO2+CD117 study (Figure 9). 40x magnification. **B)** PIEZO2 stain from PIEZO2+NF study. (Figure 9). 40x magnification. **C)** Mast cell anatomy in dura of rats. 41x magnification.

PIEZO2 cell staining data from the PIEZO2+NF study presented in Figure 8. Sample potential mast cells are identified with white arrows. Image C shows mast cells identified in the dura of a rat from a previous study¹⁶.

While Figure 9 shows co-staining between PIEZO2 and CD117, CD117 does not stain the same cell bodies that express PIEZO2. While the DAB/toluidine blue staining study does label cells of similar size and shape similar to mast cells, it is difficult to define which cells were stained by DAB and which were stained by toluidine. Therefore, we cannot confirm from that the PIEZO2 positive cells in the dura are mast cells. This observation does not necessarily rule out that the cells are mast cells, but additional studies with alternative mast cell markers will be necessary to identify them.

Section 4.3: Future Work

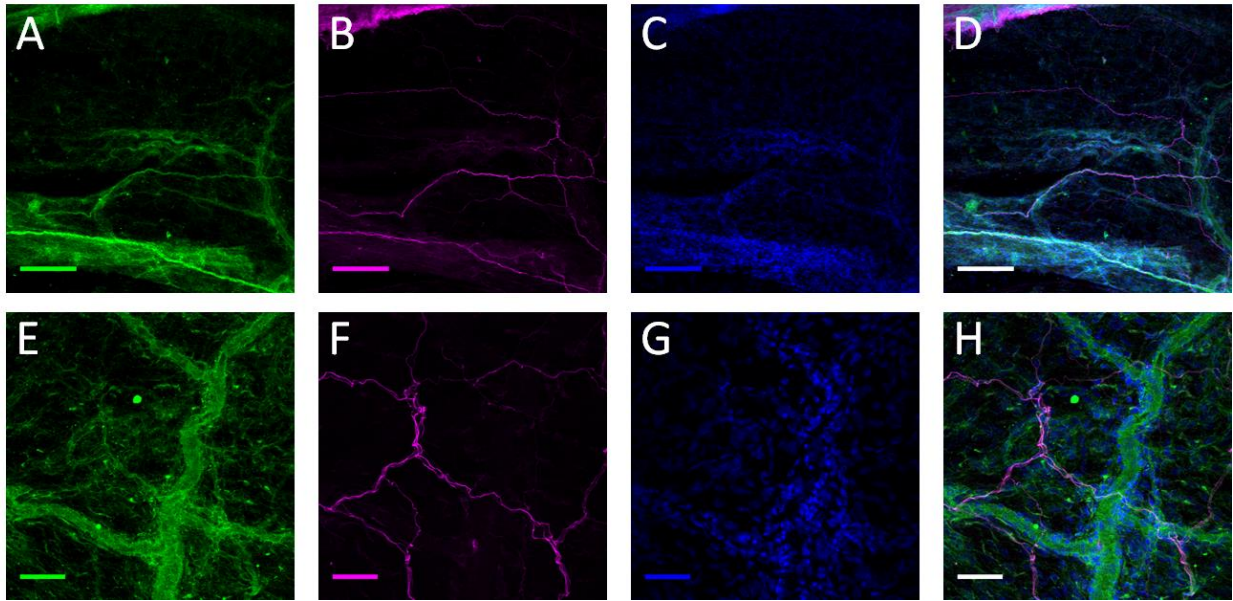
The goal of this work was to identify mechanosensory channels PIEZO1/2 in the dura to determine if they contribute to dural neurovascular coupling. While we have identified that PIEZO2 channels are present along blood vessels (specifically arteries) and axons, additional studies may be necessary to gain a more robust understanding of PIEZO1/2 activity in neurons in the dura before continuing new studies.

The next step in this project is to visualize activation and function of PIEZO channels in the dura. We can conduct in vivo studies known to activate hemodynamic forces in the vessels and observe (a) how PIEZO channels respond to the mechanical stimulus and (b) if PIEZO channels

relay this energy to adjacent neurons to produce an electrical output. We can expose the dura to shear stresses that activate the channels or conduct exercise studies in the mouse to observe the depolarization in the cell in response to the physical stimulus.

Additionally, we can relate this work more directly to migraine development by inducing migraines in a mouse model and observe changes in PIEZO channel function to understand their role in migraine formation and severity.

Supplementary Materials



Supplemental Figure 1: Immunofluorescent Staining of MAP2 and NF in the Dura

MAP2 (green), NF (pink), DAPI (blue). Scale bars 50 μ m. **A-D)** 10x Magnification. **E-H)** 40x Magnification.

1. Benatto MT, Florencio LL, Carvalho GF, et al. Cutaneous allodynia is more frequent in chronic migraine, and its presence and severity seems to be more associated with the duration of the disease. *Arq Neuropsiquiatr.* 2017. doi:10.1590/0004-282x20170015
2. Nosedá R, Burstein R. Migraine pathophysiology: Anatomy of the trigeminovascular pathway and associated neurological symptoms, cortical spreading depression, sensitization, and modulation of pain. *Pain.* ; 2013. doi:10.1016/j.pain.2013.07.021
3. Mikhailov N, Leskinen J, Fagerlund I. et al. Mechanosensitive meningeal nociception via Piezo channels: Implications for pulsatile pain in migraine? *Neuropharmacology*; 2019. doi: 10.1016/j.neuropharm.2019.02.015.
4. Gottlieb PA. A Tour de Force: The Discovery, Properties, and Function of Piezo Channels. *Curr Top Membr.* 2017. doi:10.1016/bs.ctm.2016.11.007
5. Huneau C, Benali H, Chabriat H. Investigating human neurovascular coupling using functional neuroimaging: A critical review of dynamic models. *Front Neurosci.* 2015. doi:10.3389/fnins.2015.00467
6. Mecheri B, Paris F, Lübbert H. Histological investigations on the dura mater vascular system of mice. *Acta Histochem.* 2018. doi:10.1016/j.acthis.2018.09.009
7. Drake RL, Vogl AW, Mitchell AW. *Gray's Anatomy for Students, Third Edition.*; 2015. doi:10.1017/CBO9781107415324.004
8. Nonomoura K, Woo SH, et al. Piezo2 senses airway stretch and mediates lung inflation-induced apnoea. *Nature.* 2017. doi: 10.1038/nature20793
9. Bagriantsev SN, Gracheva EO, Gallagher PG. Piezo proteins: Regulators of mechanosensation and other cellular processes. *J Biol Chem.* 2014. doi:10.1074/jbc.R114.612697
10. Saotome K, Murthy SE, Kefauver JM, Whitwam T, Patapoutian A, Ward AB. Structure of the mechanically activated ion channel Piezo1. *Nature.* 2018. doi:10.1038/nature25453
11. Parpaite T, Coste B. Piezo channels. *Curr Biol.* 2017. doi:10.1016/j.cub.2017.01.048

12. Saotome K, et al. Structure of the mechanically activated ion channel Piezo1. *Proceedings of the National Academy of Sciences*. 2014 doi:10.2210/pdb6bpz/pdb
13. Li J, Hou B, Tumova S, et al. Piezo1 integration of vascular architecture with physiological force. *Nature*. 2014. doi:10.1038/nature13701
14. Beta-Tubulin III and Neurogenesis. *Novus Biologicals*. 2016.
15. Pontén F et al. The Human Protein Atlas - a tool for pathology. *J Pathol.*; 2008.
<https://www.proteinatlas.org/search/piezo>. doi: 10.1002/path.2440
16. Dimitriadou V, Rouleau A, Trung Tuong MD, et al. Functional relationships between sensory nerve fibers and mast cells of dura mater in normal and inflammatory conditions. *Neuroscience*. 1997. doi:10.1016/S0306-4522(96)00488-5